TAO, Vol.3, No.3, 243-276, September 1992

The Year-Round Upwelling at the Shelf Break Near the Northern Tip of Taiwan as Evidenced by Chemical Hydrography

KON-KEE LIU[1,2], GWO-CHING GONG[2,3], SAULWOOD LIN[2]
CHAO-YEUH YANG[2], CHING-LING WEI[2], SU-CHENG PAI[2]
and CHONG-KUNG WU[4]

(Received: January 27, 1992; Revised: August 6, 1992)

ABSTRACT

Upwelling of the Kuroshio subsurface water at the shelf break near the northern tip of Taiwan is an important oceanic phenomenon, that results from impingement of the Kuroshio onto the continental shelf and causes profound chemical and biological responses. This upwelling region was frequently observed in the past as a pool of cold water. However, such temperature contrast does not exist throughout the year due to the cooling of the shelf water in winter. Consequently, it has never been established until now that the upwelling is a year-round phenomenon. In this study, monthly cruises were conducted from August 1990 to July 1991, and a one year-long monthly record of upwelling was evidenced from the distribution of temperature, nitrate and dissolved oxygen. The last, which revealed the structure of the upwelling dome in winter similar to those in other months, was an especially useful indicator of upwelling when temperature or nitrate concentration failed to show the whole picture of upwelling. Undersaturation of oxygen in the surface water at the upwelling center was observed during December-May. The average downward flux of oxygen in the upwelling area was computed to be 0.034 mol/m^2/day in March 1991. According to a box model for thermal and mass balance, an upwelling speed of about 5 m/day was required to maintain the oxygen-deficiency in the surface layer. The upwelling velocity yielded a total volume transport of 0.2 Sv and nitrate transport of 2x10^{9}gN/day to the top 60m in the upwelling area of 2900km^2.

[1] Institute of Earth Sciences, Academia Sinica P.O. Box 23-59, Taipei, Taiwan, R.O.C.

[2] Institute of Oceanography, National Taiwan University, Taipei, Taiwan, R.O.C.

[3] Dept. of Oceanogrpahy, National Taiwan Ocean University, Keelung, Taiwan, R.O.C.

[4] Dept. of Marine Resources, National Sun Yat-Sen University, Kaohsiung, Taiwan, R.O.C.

1. INTRODUCTION

The oceanic exchange processes at the continental shelf edge have attracted much attention in recent years due to their role in transporting terrigenous sediments and anthropogenic wastes from the shelf to the open ocean, and in supplying the shelf sea with nutrients from the deep sea (e.g., Brink, 1987; Walsh *et al.*, 1988; Wroblewski and Hofmann, 1989; Csanady, 1990). The water exchange between the shelf sea and the western boundary current has been recognized in several different modes. For example, the shelf water outflows as filaments of low salinity water (Kumpferman and Garfield, 1977; Chern *et al.*, 1990); the Gulf Stream intruded onto the continental shelf of the South Atlantic Bight by horizontal intrusion, such as over-riding or interlayering with the shelf water, or by bottom intrusion (Atkinson, 1977).

In order to investigate the temporal variation of the water characteristics at the shelf water-Kuroshio frontal region, monthly survey of hydrography and chemistry of the seawater was conducted from August 1990 to July 1991. The bottom intrusion, also termed as upwelling, was especially emphasized in the survey because of the associated shelfward nutrient fluxes. It is estimated that this process could account for 25% of the nitrate needed for the total primary production on the middle and outer shelf of the South Atlantic Bight (Dunstan and Atkinson, 1976; Yoder *et al.*, 1983; Walsh, 1991).

Upwelling also occurs along the edge of the Kuroshio, from Taiwan to Japan (Fan, 1980; Takahashi *et al.*, 1980; Liu and Pai, 1987; Su and Pan, 1987). Upwelling was often found in conjunction with the frontal eddies of the western boundary current as a result of hydrodynamic instability (Luther and Bane, 1985; Brink, 1987). Such feature varies with time and space. However, the upwelling system at the shelf break near the northern tip of Taiwan appears to be permanent (Chern *et al.*, 1990). This upwelling region has been repeatedly observed as a cold anomaly at the surface, or a subsurface dome of cold water (e.g. Fan, 1980; Liu and Pai, 1987; Chern and Wang, 1989; Wong *et al.*, 1991; Liu *et al.*, 1992). However, such temperature contrast does not exist or becomes obscure in the winter when the shelf water cools to the temperature close to or below that of the upwelled water. In this paper we demonstrate that oxygen concentration is a good indicator of upwelling under such conditions. Using chemistry as well as temperature data, we present evidences of year-round upwelling at this site, and estimated the upwelling velocity using a box model.

2. MATERIALS AND METHODS

Monthly survey of the hydrography and chemistry was conducted in the designated KEEP study area (Figure 1) on board the R/V Ocean Researcher I from August 1990 to July 1991 (Table 1), except in February 1991 when the vessel was serviced for annual inspection. The survey in July 1991 was carried out during two cruises due to the interruption of a typhoon: transect A was surveyed on cruise #288 and trasect B on cruise #289. The study area, dubbed as the P-Box, was essentially a rectangular box of 200km × 50km, trending in the NW-SE direction (Figure 1). The southwestern and northeastern boundaries of the box were designated as transects A and B, respectively. Twenty one stations were assigned on the periphery of the box. Most of the stations were evenly distributed with intervals of 25km except over the shelf break, where an additional station was inserted in each transect.

A CTD-Rosette assembly with 11 Niskin bottles was used to obtain temperature and salinity profiles and seawater samples. Water samples for dissolved oxygen, salinity and

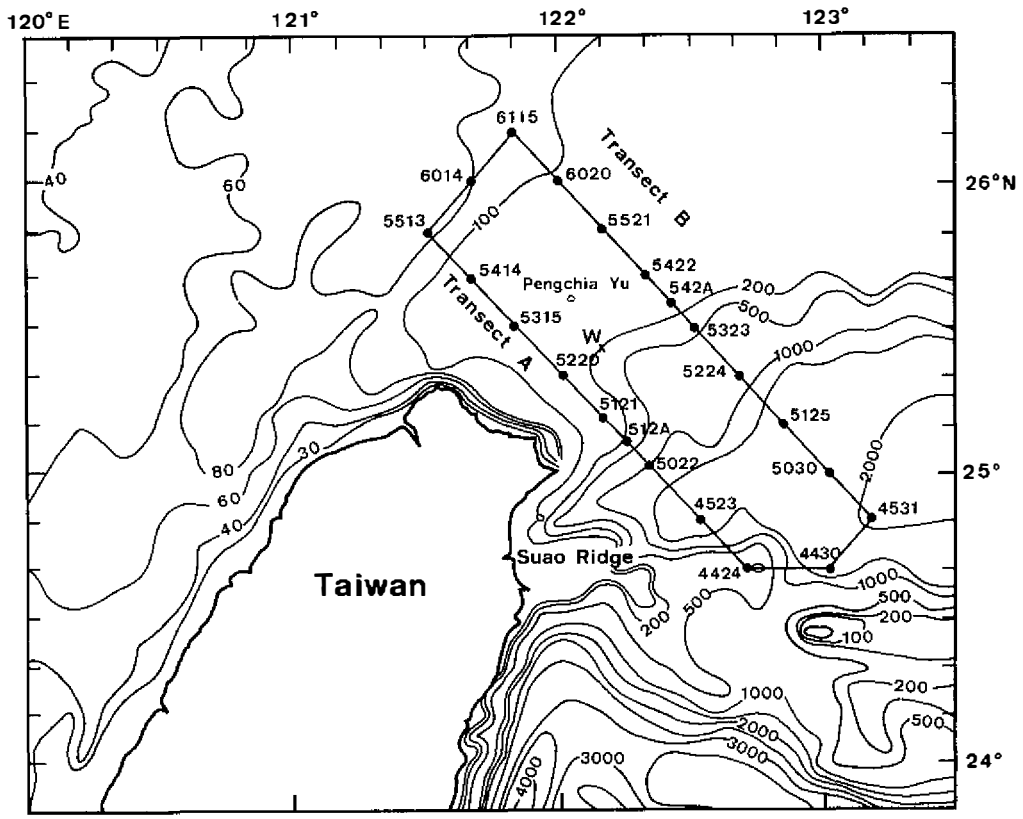

Fig. 1. Station localities of the KEEP study area. The southwestern side of the rectangle is designated the trasect A, and the northeastern transect B. Sta. W is a mooring station for current meter deployment.

nutrient determination were collected from the water samplers. The CTD unit was a SeaBird SBE11 model with an oxygen sensor. The oxygen samples were pickled immediately after collection following Carpenter's (1965) recommendation. The salinity samples were stored in 100 ml glass bottles with Poly-seal caps. The nutrient samples were frozen instantly with liquid nitrogen and stored in a freezer.

All analytical work was done shortly after the samples were returned to the laboratory. The dissolved oxygen concentration was determined not by traditional iodometric titration but by measuring the absorbance of the total iodine in the pickled samples after acidification (Pai *et al.*, 1992). The precision was $\pm 1 \mu$M. The salinity samples were analyzed with an Autosal. The salinity data from CTD were checked against the manually determined values. The frozen samples for nutrient analysis were defrosted under running water. Nitrate was analyzed with a flow injection analyzer. It was reduced to nitrite with a cadmium wire which

Table 1. Information of cruises for hydrographic and chemical survey in the KEEP study area from August 1990 to July 1991

Cruise No.	Date (Month/day/year)	No. of stations occupied
248	8/1-6/1990	21
254	9/18-23/1990	21
258	10/20-25/1990	21
260	11/3-7/1990	21
264	12/3-6/1990	10
268	1/12-15/1991	18
271	3/4-9/1991	21
275	4/1-6/1991	21
280	5/2-7/1991	17
285	6/7-12/1991	21
288	7/15-20/1991	12
289	7/22-27/1991	10

was activated with copper sulfate solution (Strickland and Parsons, 1972; Gardner *et al.*, 1976), and the nitrite was converted to pink azo dye for colorimetric determination (Pai *et al.*, 1990). The precision for nitrate analysis was $\pm 0.3\mu$M for concentrations of 10μM or higher, and better than that for lower concentrations.

3. RESULTS

3.1. Distribution of Temperature and Nitrate

A complete set of hydrographic and nitrate contour sections in the upper water column along the two transects of the KEEP study area has been published (Gong and Liu, 1991). The results from the first three cruises have been treated in a paper by Liu *et al.* (1992). Here we present the sections of temperature (Figure 2) and nitrate (Figure 3) in the upper 400m along transect B for the 11 monthly cruises which depict the monthly features of the interaction between the shelf water and the Kuroshio and provide a complete picture of the annual cycle. Transect B is chosen for presentation because it cuts closer to the center of the upwelling area. The temperature plot for the cruise of July 1991 shows only half of the transect due to loss of CTD data resulting from operational error.

The concentration of nitrate is negatively correlated with temperature in the upper water column above the oxygen minimum zone in most parts of the ocean (e.g., Craig *et al.*, 1981). Close relationships between the two were observed in the Kuroshio Water and also in the shelf water near Taiwan (Liu *et al.*, 1988; Wong *et al.*, 1991; Gong et al., 1991). A similar relationship has also been observed in the Gulf Stream (Atkinson, 1985). Consequently, the

nitrate distribution resembles that of temperature (Figures 2 and 3). Most sections showed doming of the cold nutrient-laden water at the shelf break, which is a manifestation of upwelling.

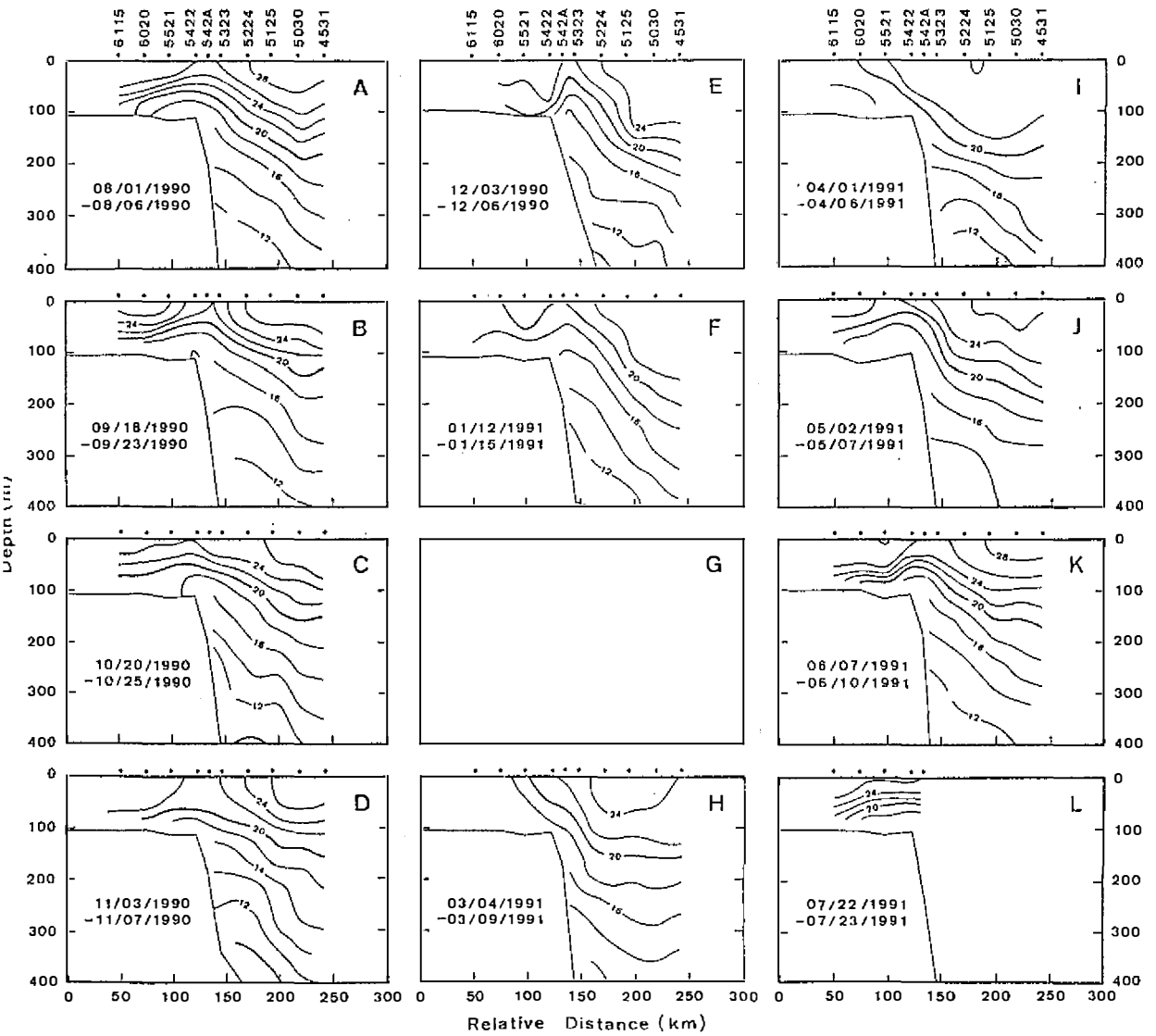

Fig. 2. The temperature sections along transect B (Fig. 1) during monthly cruises from August 1990 to July 1991.

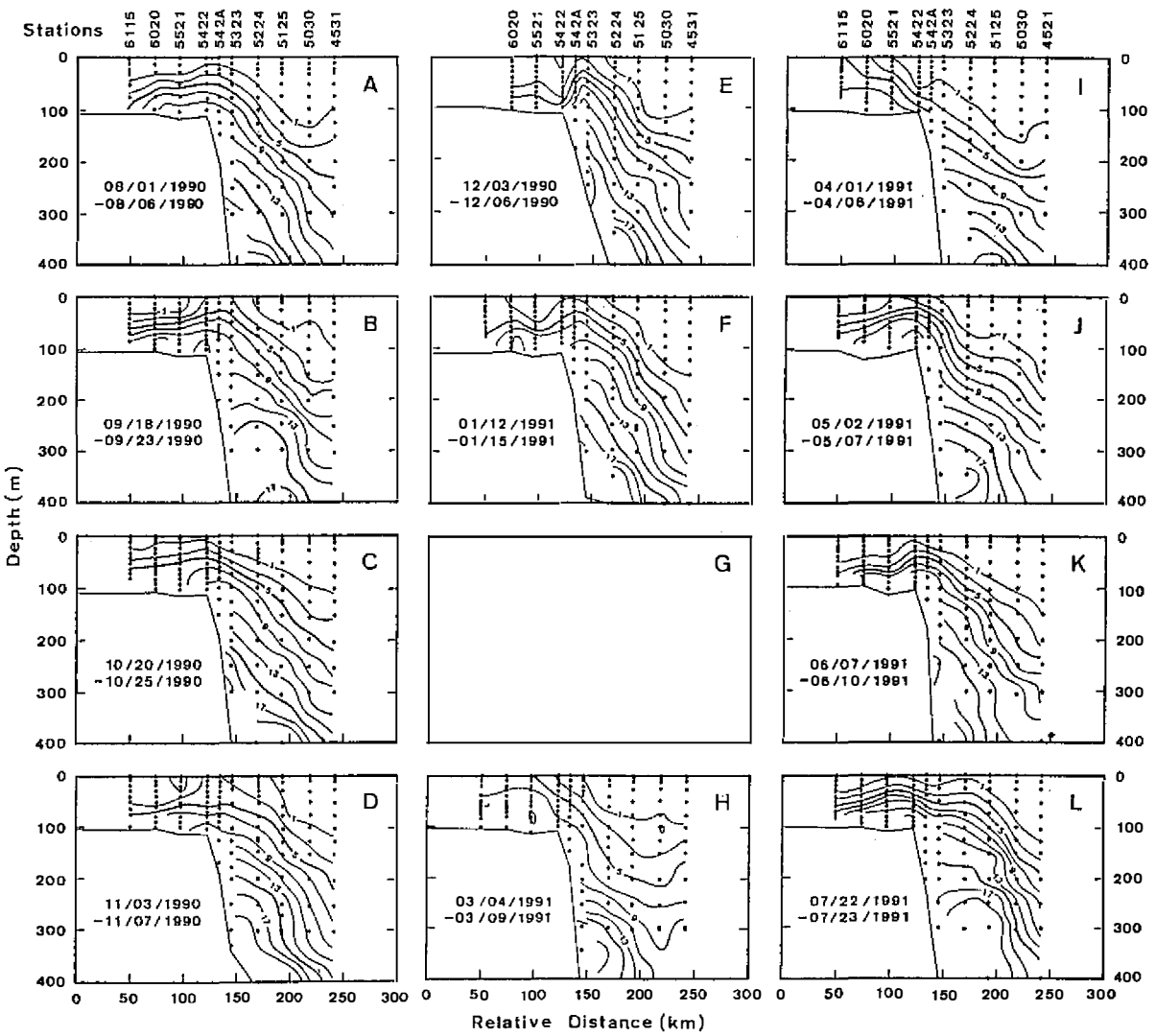

Fig. 3. The nitrate sections along transect B (Fig. 1) during monthly cruises from August 1990 to July 1991.

The relationship between nitrate and temperature in the upper water column is subject to seasonal variation due to the seasonal change of the sea surface temperature (Liu *et al.*, 1988). The sections (Figures 2 and 3) showed that the 1μM isopleth of nitrate followed the 24°C isotherm closely from May to December, whereas it follows the 22°C isotherm from January to April. From June to August the sea surface temperature was above 24°C; the surface water was devoid of nitrate. During the other months, nitrate was always present in

the surface water over the shelf break of transect B.

The distribution of temperature and nitrate in March and April 1991 appeared to be quite different from those of other months, showing only the seaward half of the dome structure. The shelfward distribution of temperature showed very small variation. The nitrate isopleths on the shelf were either horizontal or tilted upward toward the inner shelf. Although the nitrate section of transect A for the March cruise (not shown) did show a dome structure at the shelf break, the shape was not well defined. These all suggested that the distinction in temperature and nitrate between the shelf water and upwelled water was not clear in these two months.

Contrary to the aforementioned similarity between March and April, the salinities of the shelf water of the two months were clearly different (Figure 4). In March, water of very low salinity (33.6 psu) was pressing against the high salinity water (34.6 psu); whereas, in April, the salinity of the shelf water (mostly within 34.4-34.7 psu) was more uniform and considerably higher than that in March.

The nutrient-deficient surface water from the West Philippine Sea extended more deeply onto the shelf in April 1991 than in October 1990. All sections showed a tongue of cool ($<18^{\circ}C$) and nitrate-rich ($>7\mu M$) water extending from the open sea up the slope and toward the shelf break, except the section of April. In April, the tongue was interrupted by a thick layer of nitrate-depleted water and the nitrate isopleths sank considerably in the water off the shelf break.

3.2 Distribution of Dissolved Oxygen

Determination of dissolved oxygen was not satisfactory on the first few cruises due to storage problems and procedural complexity of the potentiometric end point detection. Satisfactory analysis was not obtained until the spectrophotometric measurement of the total iodine for the oxygen determination developed by Pai *et al.* (1992) was adopted in December 1990. Figure 5 shows the oxygen data from December 1990 to June 1991. The oxygen data for July 1991 was missing due to operational difficulties under bad weather. Similar to the temperature and nitrate sections, the oxygen sections also show the prominent dome structure at the shelf break. However, in March and April 1990 when the dome structure in the temperature and nitrate distribution was incomplete, the oxygen section showed a complete dome structure.

Comparison of the oxygen sections of March and April, 1991 revealed considerable difference in the dome structure of upwelling, reflecting the different hydrographic conditions. In March, very sharp contrast of oxygen concentration was observed on the shelfward half of the dome structure, with the highest concentration above $250\mu M$ and the lowest concentration below $195\mu M$. The oxygen isopleths of the shelf water rose steeply near the center of upwelling. In April, the sharp horizontal oxygen gradient in the shelf water disappeared, and the isopleths of the shelf water were essentially horizontal except near the upwelling center.

3.3 Sea Surface Temperature and Meteorological conditions

Figure 6A shows the annual variation of air temperature and sea surface temperatures (SSTs) in different regions in the KEEP study area. The thermal boundary between the Kuroshio Water and the shelf water fluctuated in a wide range across the outer shelf off northeastern Taiwan (C.-Y. Lin *et al.*, this issue). According to the satellite imageries of SST, the three deepest stations (namely, 4430, 4531 and 5030) were on the seaward side of

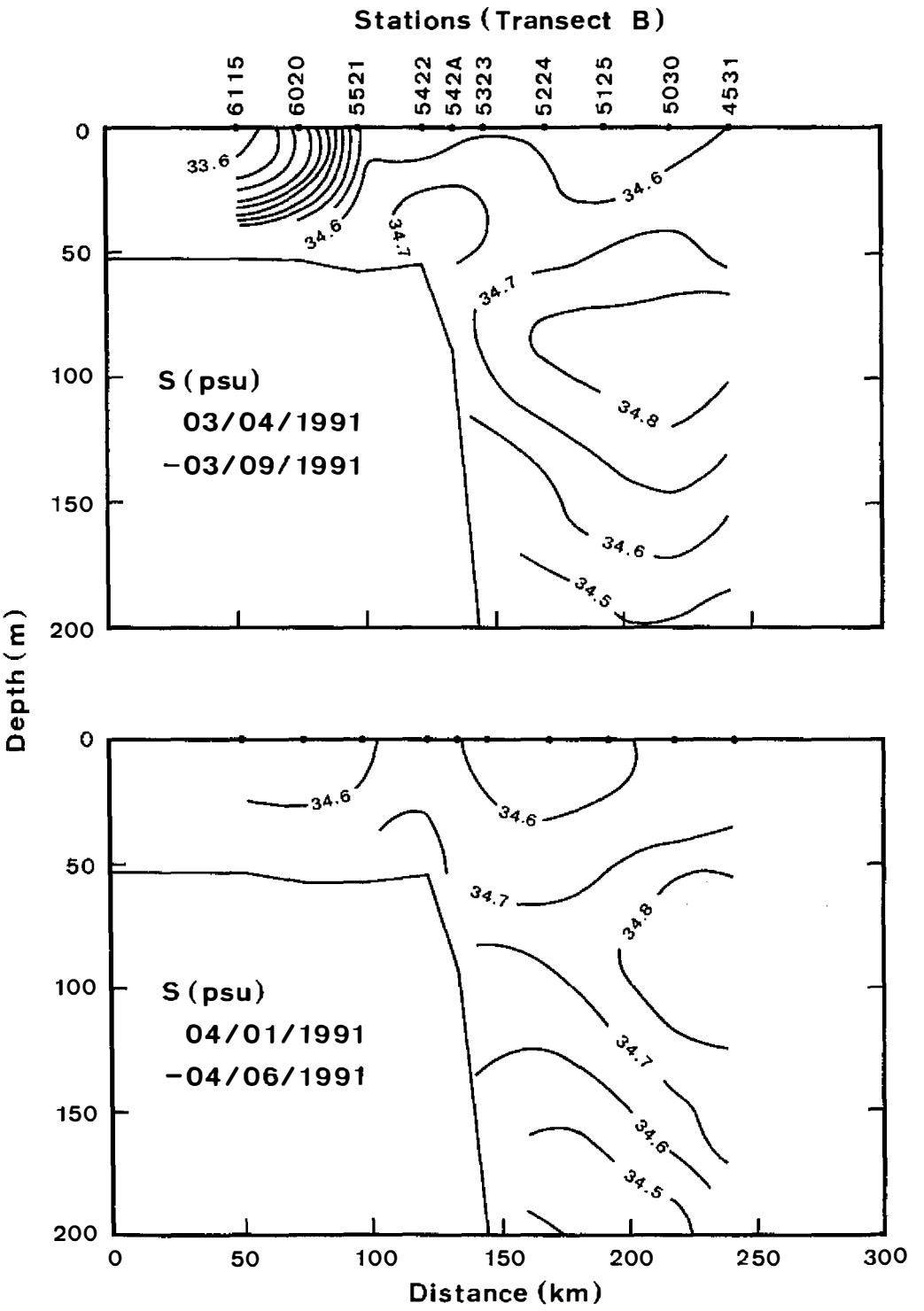

Fig. 4. The salinity sections along transect B (Fig. 1) observed during the cruises in March (upper) and April (lower), 1991.

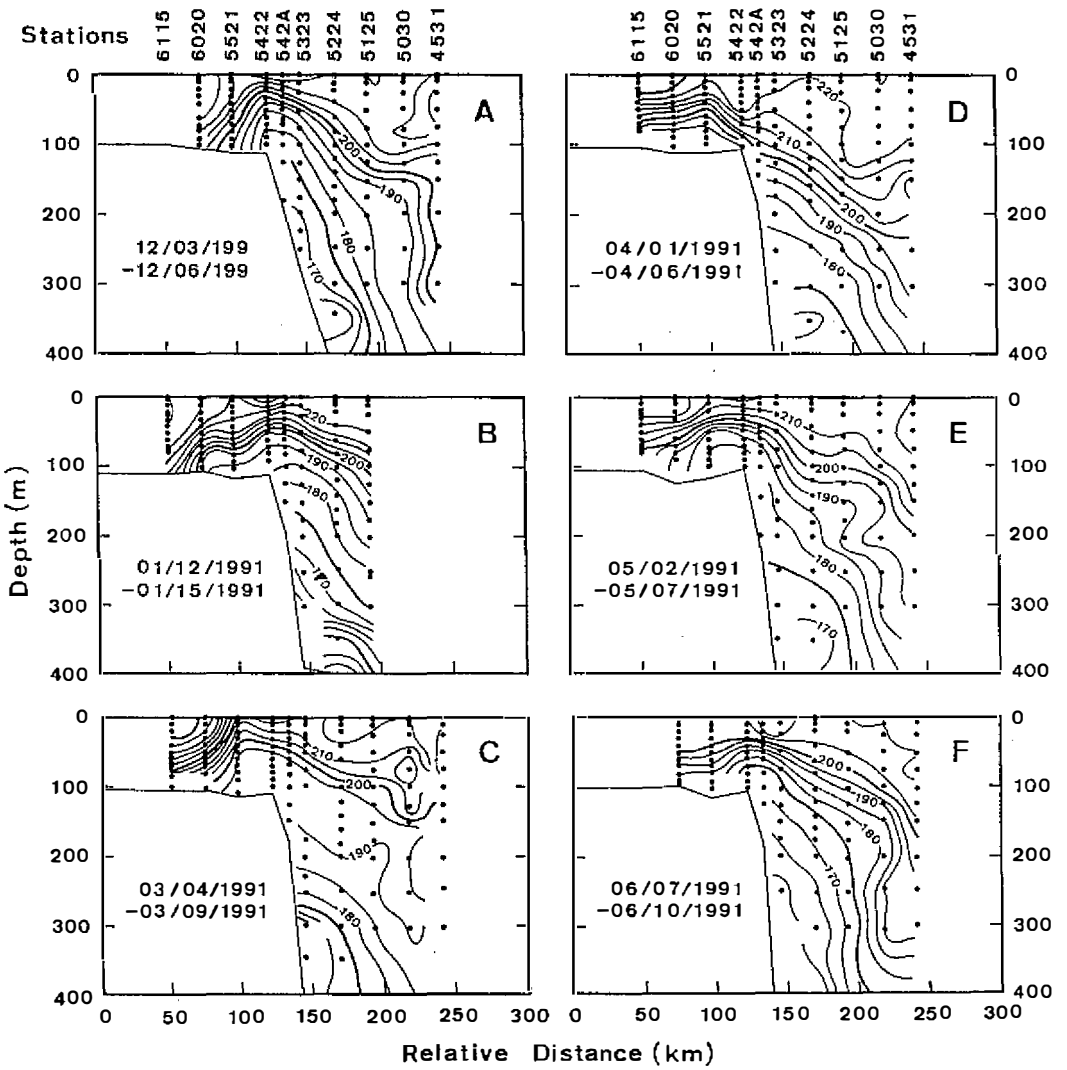

Fig. 5. The section contours of dissolved oxygen along transect B (Fig. 1) during monthly cruises from December 1990 to June 1991.

the front, while the three innermost stations (namely, 5513, 6014 and 6115) were on the shoreward side of the front most of the time. Therefore, these two groups of stations are used to represent the surface conditions of the deep and the shelf seas, respectively. The station at the crest of the upwelling dome in the temperature or oxygen sections represents the upwelling center. The air temperature is the 7-day mean at the Pengchia Yu Island. It is noted that the altitude of the weather station is 100m above sea level. The air temperatures at

the station should be lower than that near the sea surface. The mean difference was probably within 1°C as inferred from the mean adiabatic lapse rate of the troposphere: 6.5°C/km (Goody and Walker, 1972). Such difference is small, compared to the fluctuation of the air temperature.

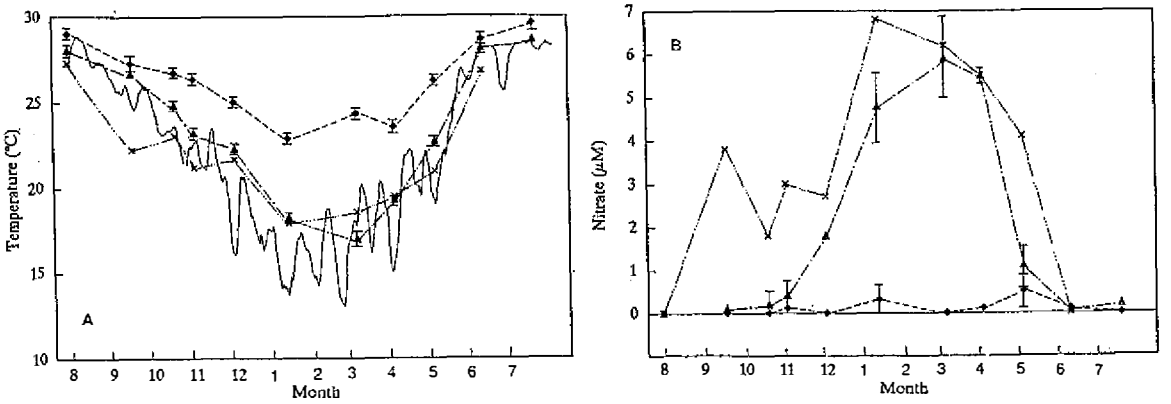

Fig. 6. (A) Variation of sea surface temperature in the open ocean (diamonds), the inner shelf (triangles) and the upwelling region (crosses) as observed during the hydrographic survey from August 1990 to July 1991. The vertical bars represent the standard variation among the representative stations (see text). Also shown is the air temperature variation (smoothed by 7-day running mean) on the Pengchia Yu Island during the same period. (B) The same as (A) except for nitrate.

Figure 7A shows the time series of the 10-day low passed (10-DLP) wind velocity observed at Penghu and Pengchia Yu, in 1990 and 1991. Although the wind velocity at Pengchia Yu was more variable than at Penghu, the transitions of the prevailing wind directions observed at the two sites were almost synchronous during our study period. The onset of the northeast monsoon in 1990 occurred in mid-September. The reversal back to southerly wind in 1991 occurred in mid-May. Time series of the daily mean wind velocity from February 1 to April 30, 1991 is shown in Figure 7B. The wind conditions were correlated with the unusual hydrography observed in March and April, 1990 (see Discussion).

The SST over the shelf followed the trend of air temperature quite closely. The air temperature reached a maximum in August and started to drop in September; it reached the lowest point in February and started to rise in March. From September to mid-November, the surface temperature of the shelf sea was about equal to the mean air temperature. When the air temperature started to show cold surges, the sea surface temperature stayed near the upper limit of the air temperature. During the warming period from March to June, the sea surface temperature was approximately equal to the mean level of the air temperature. Therefore, the change of the sea surface temperature appeared to lag behind change of the air temperature.

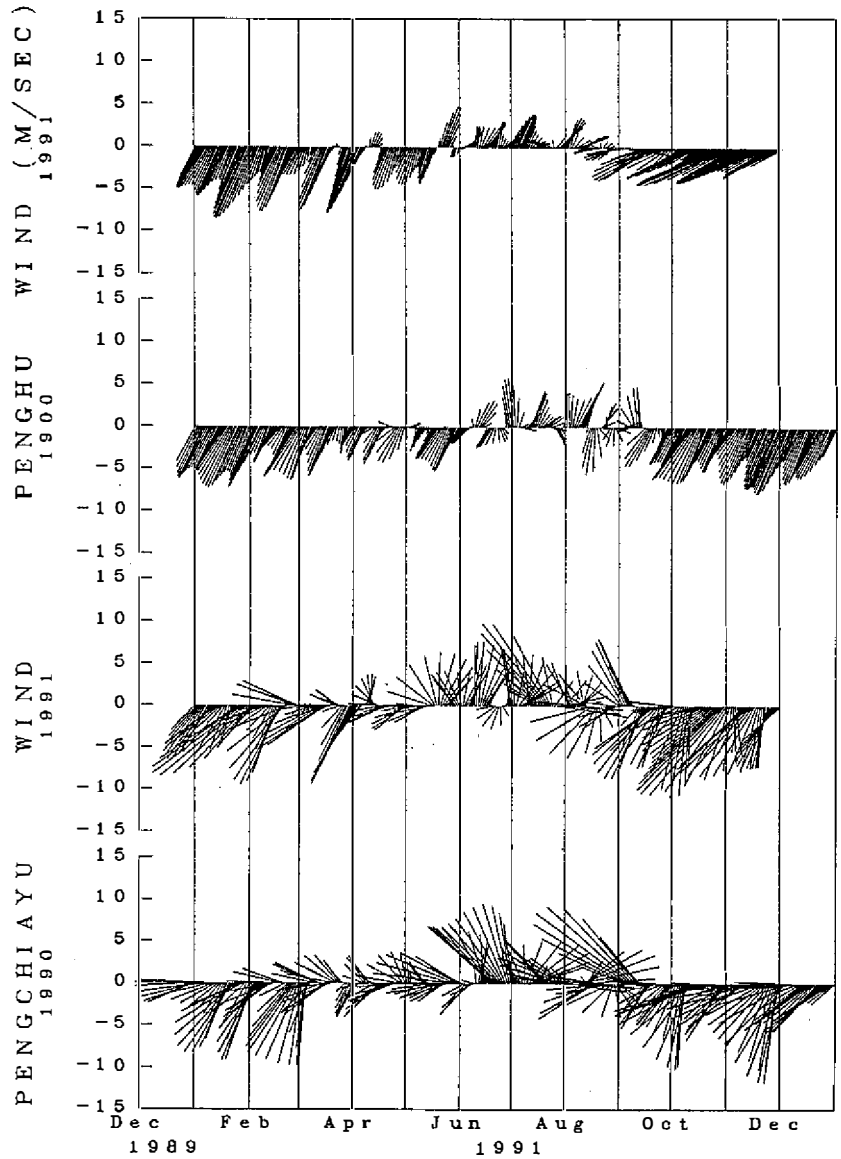

Fig. 7A. Time series of 10-DLP wind velocity observed at Penghu (upper two panels) and Pengchia Yu (lower two panels), from January 1990 and to November 1991. The onset of the NE monsoon occurred in mid-September in both years. The onsets at the two sites were synchronous.

The surface water of the open sea was slightly warmer than the shelf sea by less than 2°C from June to September. After September, it also cooled down but with a slower rate,

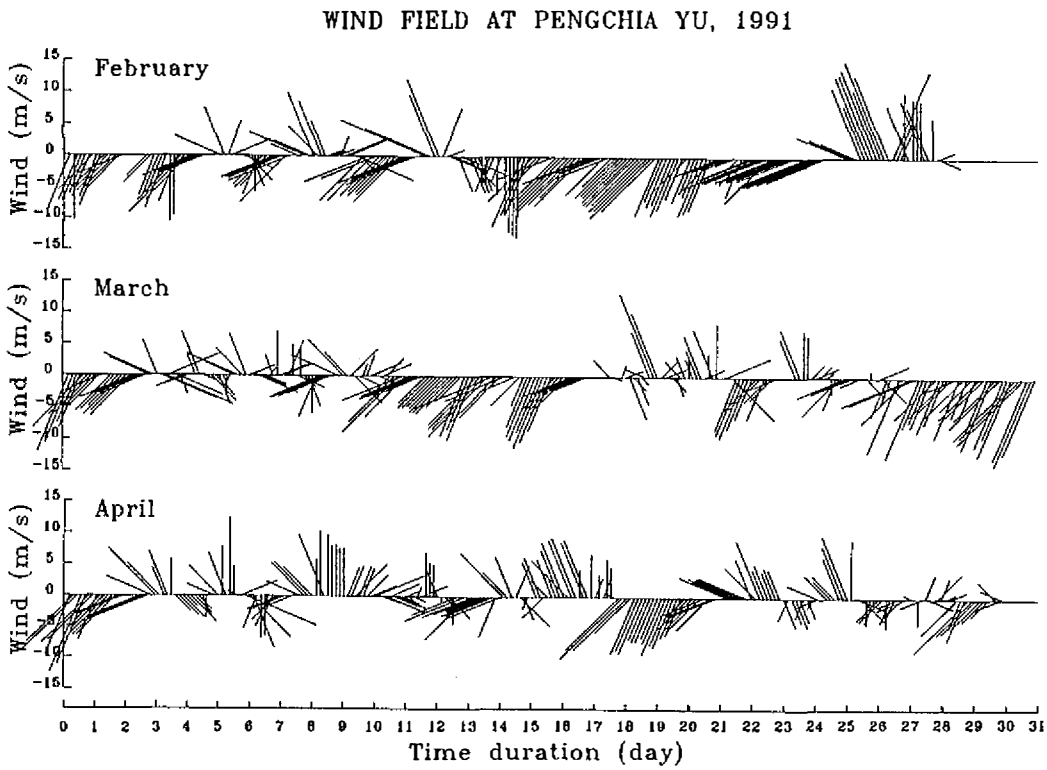

Fig. 7B. Time series of daily mean wind velocity observed on Pengchia Yu from February 1 to April 30, 1991.

and then stayed around 23°C through winter (Figure 6A). Warming began after April. The surface water of the upwelling center was cooler than the shelf water from August to November and from May to July. During the same periods of time, the upwelling center was also cooler than the mean air temperature, indicating that the cold anomaly was attributable only to upwelling. The most intense cold anomaly was observed in September 1990, corresponding to the onset of northeast monsoon (Liu *et al.*, 1992). From December to April, the observed surface temperature of the upwelling center was very close to or even higher than the shelf water. However, it should be noted that the observed upwelling center did not necessarily coincide with the true center of upwelling because the cruise track might have missed the apex of the upwelling dome. Therefore, the lack of evidence of cold anomaly in winter did not ruled out its existence, but the contrast would be much smaller than in autumn if it had existed.

4. DISCUSSION

There are two types of water transport from the Kuroshio onto the shelf: upwelling and intrusion. The former represents ascending of the thermocline water of the Kuroshio to the shelf. The latter represents mostly lateral movement of the upper Kuroshio Water of high

salinity onto the shelf (Liu *et al.*, 1992). The upwelling at the shelf break off the northern tip of Taiwan is important not only for the nutrient budget of the East China Sea but also for its revelation of the hydrodynamic response of the Kuroshio circulation to the regional bottom topography. The volume transport of upwelling needs to be quantified for estimation of the nutrient flux, but the complexity of the upwelling system is formidable for such approach. Nevertheless, we would like to discuss the influence of the physical parameters on the chemical hydrography of the upwelling system, and to estimate its strength using a box model.

4.1 Influence of Meteorological Conditions on Hydrography

It has been demonstrated that the upwelled water is contrasted with the surface water most notably by the differences in temperature, and concentrations of nutrients (e.g., Liu and Pai, 1987; Wong *et al.*, 1991; Liu *et al.*, 1992). However, the observations in March and April, 1991 indicated that temperature and nutrient concentration of the upwelled water were not distinctive from the shelf water which was also cool and laden with nutrients. Instead, oxygen could be an auxiliary indicator of upwelling. Before exploiting the usefulness of oxygen, we would discuss the hydrographic conditions observed on the two cruises.

The contrasting hydrographic conditions observed in March and April 1991, were probably related to the wind conditions. The low salinity water observed in March most likely came from northern Taiwan Strait which is the nearest area with low salinity (with a mean of 33.4 psu) in winter (Hwang and Tang, 1992). Similar distribution of the water mass was observed by Chern and Wang (1989). One week prior to the March cruise, wind changed from NE to southerly with only temporary reversal (Figure 7B). Although the wind in Penghu did not reverse, the strength did decrease to less than half before the March cruise (Figure 7A). According to Chern and Wang (personal communication, 1992), the NTS Water would spread northward when the NE monsoon relaxed. The low salinity constituent of the NTS Water was most likely from the Continental Coast Water which contains a large fraction of the Yangtze River runoff (Miao and Yu, 1990). The possibility of the low salinity water originating from the south should be dismissed because the salinity distribution showed increase toward the south in winter (Tang and Chen, 1990).

The salinity of the shelf water observed along transect B in April was uniformly high (with a mean around 34.6 psu) as compared to the mean salinity of 34.35 psu in the outer shelf off northern Taiwan (Hwang and Tang, 1992). The most likely source of the high salinity water was the Kuroshio Water which had mean salinity of 34.5-34.7 psu in the top 150m at the slope off northeastern Taiwan in the spring (Hwang and Tang, 1992). Therefore, the hydrographic conditions observed in April suggested onshore movement of the top layer of the Kuroshio Water. In addition, the shelfward expansion of the nitrate-depleted layer also lent support to the Kuroshio intrusion, because the surface Kuroshio Water is usually devoid of nitrate (Liu *et al.*, 1988). On the other hand, the NTS Water had mean salinity less than 34.4 psu in the spring, and its surface concentration of nitrate has been observed at 3μM or higher (Fujian Institute of Oceanology, 1988). Therefore, the NTS Water was an unlikely source for the high salinity water on the outer shelf.

The satellite SST imagery obtained on April 10, 1991 also indicated shelfward expansion of the warm Kuroshio Water. The thermal boundary extended shelfward beyond 122°E and passed between stations 5220 and 5315 along transect A and between stations 6020 and 6115 along transect B. The Kuroshio intrusion in April was similar to that in October 1990 (Liu

et al., 1992) but more extensive. Before the April cruise (April 1-6), the NE monsoon had been persistent for a week (Figure 7B), which probably assisted the Kuroshio intrusion onto the shelf, but other factors, such as outflowing of the inner shelf water in the previous month or remote forcing, could also be important.

The current meter records at station W (25° 25.40′N, 122°7.70′E, 270m deep) near the shelf break (Figure 1) indicated that the slope water also moved towards the shelf at the same time as the April cruise. The deployment of the current meters were described by Chuang and Wu (1992). The progressive vector plot of the low passed data of current meter at depths of 190m and 245m showed changes of drift direction from southwestward to, respectively, westward and northwestward at the end of March 1991 (Figure 8). The temperatures recorded at the two current meters rose gradually from about 15 to 16.5°C and from 14.5 to 15.5°C, respectively, between March 20 and April 9 (NSC, 1991). Such records suggested movement of the Kuroshio Water towards the shelf.

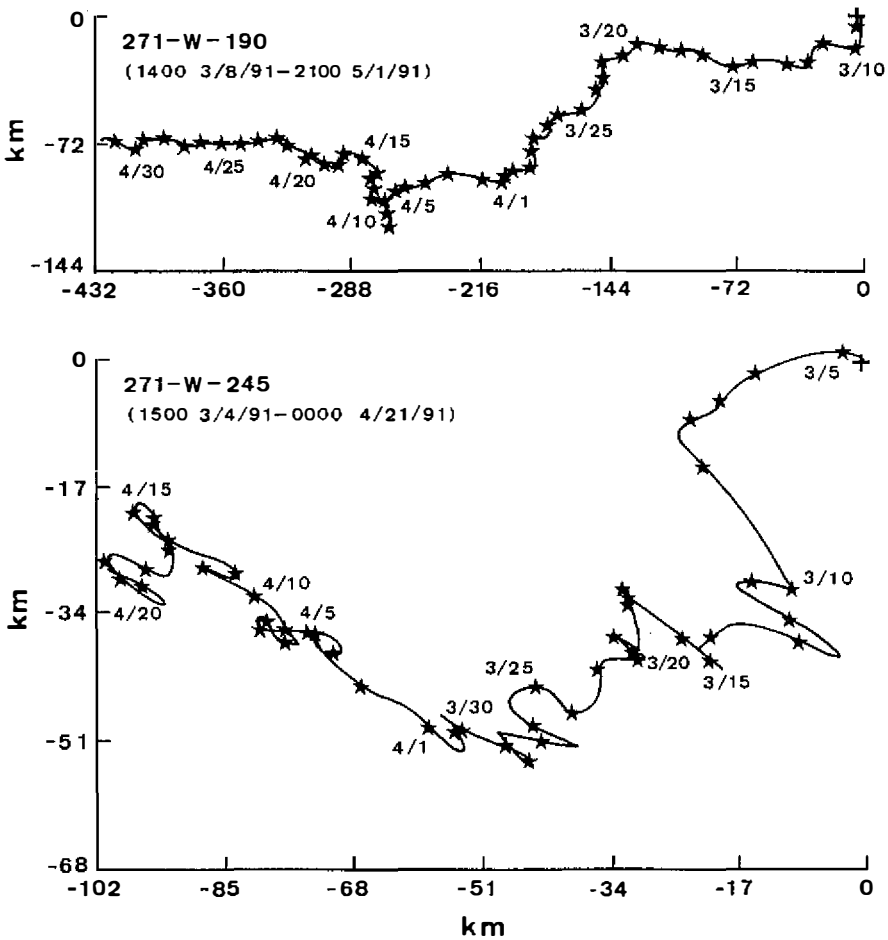

Fig. 8. The progressive vector plot of the low passed current meter records at mooring station W (water depth =270m) on the shelf break. The cross indicates the beginning of the record. The star indicates the beginning of each day. (A) The record at 190 m below sea surface from March 8 to May 1, 1991. (B) The record at 245 m below surface from March 4 to April 21, 1991

4.2 Manifestation of Upwelling

The manifestation of upwelling is characterized by the contrast between the upwelled water and the shelf water. Because the upwelled water is immediately mixed with the shelf water as soon as it reached the shelf due to internal motion (Chern and Wang, 1990; Liu *et al.*, 1992), the signal of upwelling is soon dispersed if the upwelled water is not supplied continually. The intensity of the manifestation is controlled not only by the strength of upwelling but also by the efficiency of mixing and the difference in water characteristics between the upwelled water and the shelf water. In addition, the circulation pattern which controls the residence time of the upwelled water at the shelf break also affects the signal of upwelling. In light of these processes, we will discuss the usefulness of dissolved oxygen concentration as an upwelling indicator. It is easy to understand that the contrast in temperature between the shelf water and the upwelled water vanished in the cold months when the shelf water became cooler than the upwelled water. However, in March and April , the contrast in nitrate concentration also became indistinguishable, and dissolved oxygen became the only distinctive indicator.

In addition to oxygen distribution, the degree of oxygen saturation also testified to upwelling. Figure 9 shows the degree of oxygen saturation in transect B in March and June, 1991, respectively. The surface layer of about 30m in both the shelf water and the deep sea was saturated with oxygen, except in the upwelling dome. In March, the surface water at the upwelling center was undersaturated with oxygen by 7%. Such a phenomenon was also observed on other cruises from December to May. In the upwelling dome, freshly upwelled water must contribute to the mixed layer. Otherwise, it would be saturated with oxygen rapidly.

In March, the NTS Water pressed against the upwelled Kuroshio Water at the shelf break. The nitrate distribution indicated that the NTS Water was laden with nitrate. There are three reasons for the presence of high nitrate concentration at the surface of the inner shelf water: (1) strong vertical mixing, (2) reduced biological uptake, and (3) contribution from the CCW. In winter and early spring, the NTS Water resembles inner shelf waters in the southern East China Sea which are vertically well mixed and destratified in the cold seasons (Chern and Wang, 1989; Miao and Yu, 1990). The turn-over of the shelf water brings nutrients in the bottom water to the surface. The biological uptake of nutrient was weaker as indicated by the lower chlorophyll-a concentration in the upwelling area in March than in other months (Chen, Y.-L., 1992). The lower primary productivity in the shelf water was probably due to lower temperature and stronger vertical mixing in winter (Parsons *et al.*, 1984). The low salinity constituent of the NTS Water, i.e., the Continental Coast Water, which contains significant amounts of nutrients and particulate matter (Edmond *et al.*, 1985; Fujian Institute of Oceanology, 1988), may also contribute to the nutrient loading.

Destratification and reduced biological production are especially important in decoupling the oxygen and nutrient behavior in seawater. Under normal conditions, the increase of nutrient is associated with depletion in oxygen, and vice versa. The increase of nutrient usually results from nutrient regeneration, which consumes oxygen. On the other hand, the increase of oxygen results either from photosynthesis or from ventilation. During photosynthesis nutrients are always consumed, but during ventilation, which means air-sea exchange at the surface, nutrients may or may not be depleted, depending on the rate of primary production. In the cases observed in March and April, the high concentration of nutrients in the surface water on the shelf was obviously a consequence of low primary productivity and

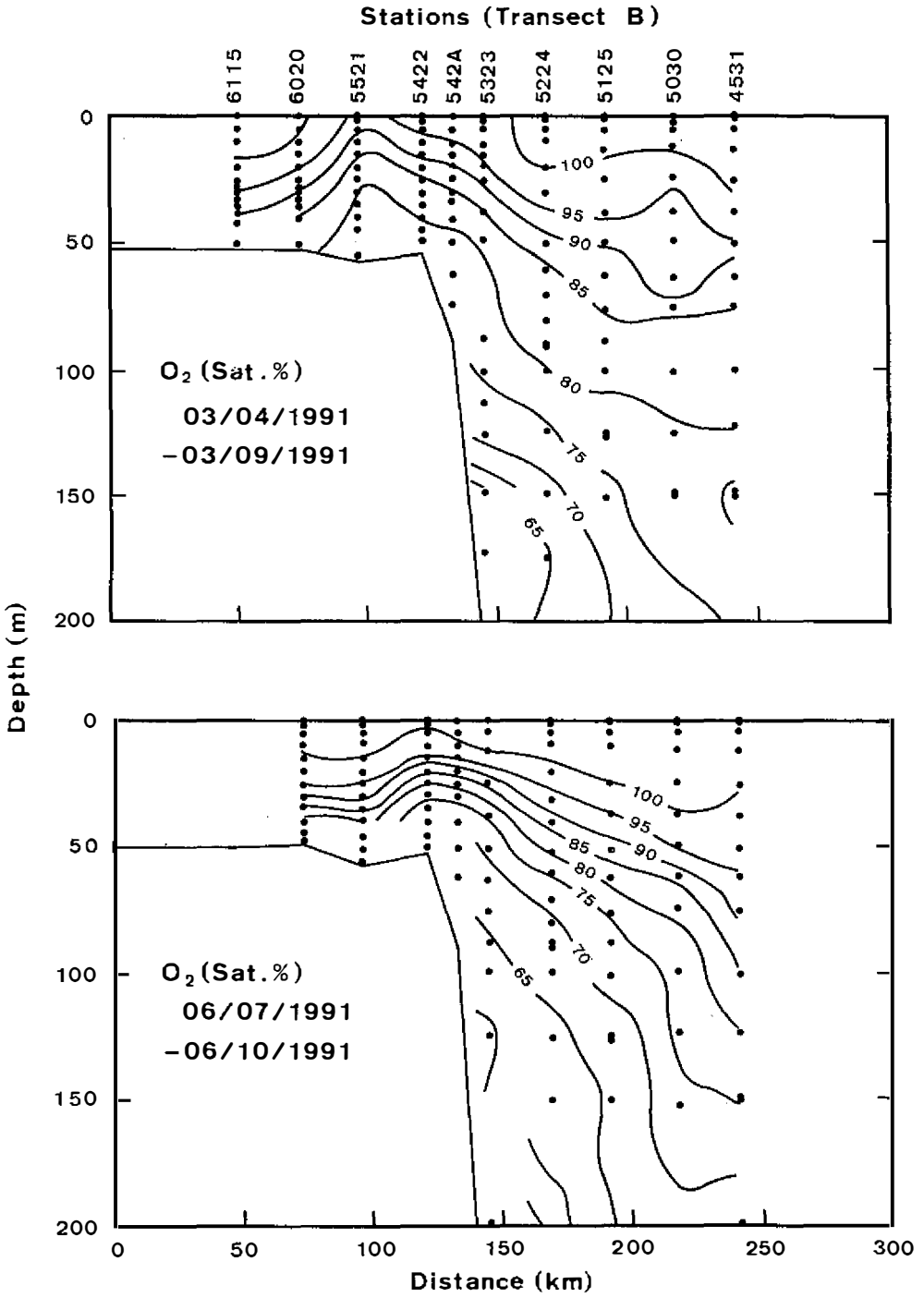

Fig. 9. Section of the degree of oxygen saturation along transect B during the cruises in March and June, 1991. Undersaturation of oxygen in the surface water of the upwelling center was observed in March 1991.

active vertical mixing, while the oxygen in the surface water was replenished fast enough to reach saturation, except in the upwelling center where vertical supply of undersaturated water must be faster than the dissolution rate. It is interesting to note that the distinction in temperature and nitrate between the shelf water and the upwelled water did not fade or disappear in January, which was much colder than April (Figure 6A). This actually supported the role of destratification in affecting the shelf water properties and the behavior of nitrate and oxygen. Destratification of the shelf water, which usually lagged behind the temperature change, probably was not well developed in January but was in March and April.

The usefulness of the dissolved oxygen as an indicator of upwelling is limited only to cold periods. In March, the shelf water was colder than the Kuroshio surface water and, therefore, contained high concentration of oxygen (up to 250μM). Such high oxygen concentration made the shelf water distinctive from the upwelled water which is depleted in oxygen. The contrast in oxygen concentration between the upwelled water and the shelf water became more noticeable due to the increased oxygen solubility at lower temperature. In the summer, the low oxygen solubility in the much warmer surface water does not provide enough contrast from the upwelled water and can not be used as an upwelling indicator. In June all the surface water, including the upwelling center, was saturated with oxygen (Figure 9). Such change may be attributable to decreased upwelling intensity and the increased temperature; the latter lowered the oxygen solubility and hasten dissolution. These factors made the upwelled water lose its signature of oxygen depletion quickly. The lower vertical diffusivity and the biological production of oxygen were additional factors which may contribute to the situation.

Using different indicators, we were able to establish that the upwelling dome existed throughout the year. From December to April, the upwelling center was characterized by the doming of oxygen isopleths; during other months, it was by the doming of isotherms. It should be noted that the observed dome structure did not reflect reality precisely but was slightly distorted by tidal and internal motion of the shelf water during the sampling period. The maximum horizontal displacement due to semi-diurnal tide was calculated to be 5-13km for the top 90m (Lee, 1992). The major features of the dome structure were readily identifiable but the detailed features were difficult to interpret. Basically the structure consists of a major dome at the shelf break, which was more or less symmetric with a few exceptions. Occasionally, there was a minor dome to the shelfward side (January 1991) or to the seaward side (July 1991). In some other occasions, e.g., October 1990 and April 1991, the shelfward side of the dome structure showed rather flat isopleths, which were possibly caused by the circulation pattern near the shelf break during Kuroshio intrusion. The center of the upwelling region, which is presumably indicated by the crest of the dome, was located mostly at the shelf break but with occasional displacement slightly seaward or shelfward. Such displacement never exceeded 25km from the shelf break. The mean position of the upwelling center appeared to be locked at the shelf break. The year-long record confirmed the claim of Chern *et al.* (1990) that upwelling is a permanent feature in this region.

It is noteworthy that the nitrate section of July 1991 (Figure 3L) showed an additional doming region about 50km seaward from the shelf break. At the same time, the 19μM isopleth of nitrate was uplifted notably to the depth of less than 300m in the region off the shelf. Before the July cruise, typhoon Amy passed through southern Taiwan on the 18th. After entering the South China Sea on the 19th, it caused strong southerly wind in the KEEP study area . During the hydrographic survey on the 22th and 23rd, there was typhoon Brenda which was passing through the Bashi Channel, and caused southeasterly wind in the KEEP

study area. Their records are visible in Figure 7A. It is not clear whether the unusual features were directly related to the typhoons.

4.3 Controls on Nitrate Distribution

The variation of nitrate concentration in the surface layer, where the biological production is most active, was closely related with the meteorological conditions (Figure 6). In the shelf water, the surface concentration of nitrate was essentially zero from June to September, which corresponded to the period of southeast monsoon. The nitrate concentration started to increase rapidly in November and reached a maximum of 61μM in March. The nitrate variation was the inverse of the temperature variation. Aside from the intensification of upwelling, the reason for the increase of nitrate in the shelf water during the months of prevailing NE monsoon are similar to those for the inner shelf water. However, the mixing process is probably the most important factor in controlling nitrate distribution (Liu *et al.*, 1988). The relationship between temperature and nitrate appeared to result from mixing between the nitrate-depleted surface water and the upwelling source water. Because upwelling is a year-round phenomenon, the upwelling source water can be considered as a constant end member. The properties of the other end member are apparently dependent on the meteorological conditions. Because the SST of the shelf water followed the air temperature quite closely, those properties of the surface end member could be derived. Then, the nitrate distribution in the shelf water can be determined from the temperature distribution which is much easier to measure than the nitrate.

The nitrate concentration in the surface water of the upwelling center was the highest among the three types of regions; it nevertheless decreased to the non-detectable level during the summer (June to August). The first appearance of significant concentration of nitrate (up to 4μM) in surface water at the upwelling center in autumn was coupled with the abrupt temperature drop ten days after reversal of the prevailing wind direction in September (Liu *et al.*, 1992). This is a possible sign of intensification of upwelling which has been demonstrated as a plausible response to the onset of NE monsoon by dynamic modeling. Its variation was not as smooth as the shelf water probably because its value was sensitive to the position of sampling site relative to the true upwelling center. On the other hand, the variation may also be attributable to other factors, such as the variable intensity of upwelling. Although the sampling stations did not necessarily occupy the true upwelling center, the nitrate concentration at the "upwelling center" observed on transect B was still higher or equal to that of the shelf water. In March the sea surface temperature of the upwelling center was higher than that of the shelf water, but the nitrate concentrations were about the same. The nitrate anomaly clearly demonstrated that upwelling was an important source of nitrate.

In contrast to the shelf water, the nitrate concentration in the surface water of the deeper area remained low (below 0.5μM) throughout the year (Figure 6B), and was at non-detectable levels from June to October. During the period while the shelf water was rich in nitrate, detectable concentration of nitrate appeared occasionally in the surface water of the deeper area, suggesting that nutrients were possibly transported from the shelf to the Kuroshio Water by episodic occurrences of filaments which had been observed twice during the onset of NE monsoon (Chern *et al.*, 1990; Liu *et al.*, 1992).

4.4 Oxygen Flux at Sea Surface

The undersaturation of oxygen in the surface sea water indicated rapid removal of oxygen from the sea surface by diffusion or continual replacement of the surface water by

the underlying oxygen-depleted water. The condition observed at sta. 5521 on the shelf break during the March cruise was used as an example to calculate the oxygen flux at sea surface by diffusion.

The temperature profile (Figure 10) at this station indicated that the water column was divided into three layers. The waters in the top 10m and below 60m were rather uniform, while the middle layer showed a marked thermal gradient. The oxygen profile was similar to the temperature profile except that the top layer showed a noticeable negative gradient in oxygen (Figure 10), suggesting that the exchange of oxygen at the sea surface was more pronounced than the thermal exchange.

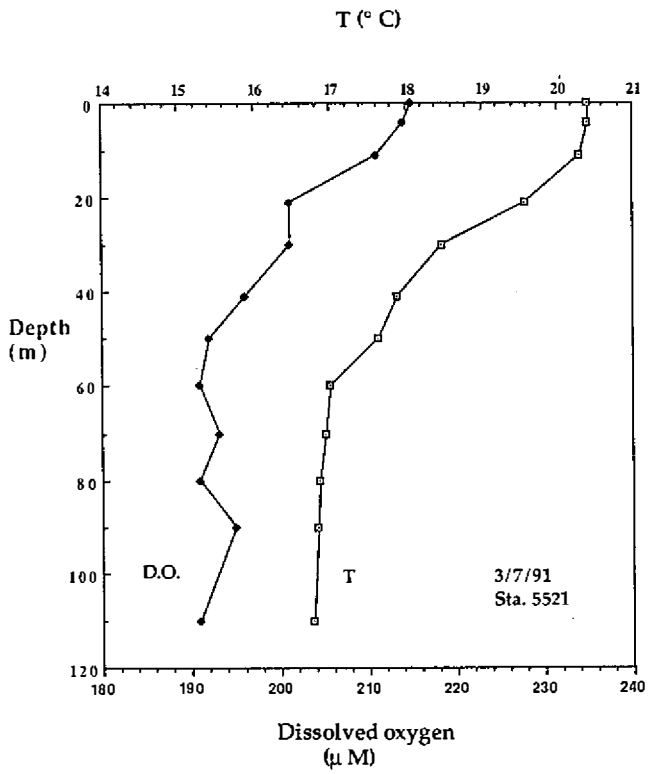

Fig. 10. Profiles of temperature and dissolved oxygen concentration observed on March 7, 1991 at sta. 5521.

The flux of oxygen (F) transported from the atmosphere to the surface seawater can be calculated from the degree of oxygen saturation and the exchange coefficient (Kester, 1975):

$$F = K \times (Csatd - Cs) \tag{1}$$

where K is the exchange coefficient of oxygen, $Csatd$ is the concentration of oxygen in seawater in equilibrium with the atmosphere, and Cs is the oxygen concentration at sea surface. The saturated oxygen concentration at the surface T-S condition (20.4°C and 34.58

psu) was calculated to be 229μM (Weiss, 1970), while the observed oxygen concentration was 215μM. The exchange coefficient can be expressed as

$$K = D_{O2}/Film, \tag{2}$$

where D_{O2} is the diffusivity of oxygen in seawater and "$Film$" is the thickness of the surface laminar layer, which is also termed the stagnant film (Broecker and Peng, 1974). D_{O2} is 2.08×10^{-5} cm^2/sec for oxygen at 20.4°C (Broecker and Peng, 1974). The global mean value of the stagnant film thickness was estimated to be 30μ from ^{14}C exchange and 36μ from radon deficiency in surface sea water (Peng *et al.*, 1979). In principle, the value of the stagnant film thickness is dependent on wind speed (Broecker and Peng, 1974; Wanninkhof *et al.*, 1985) but the relationship is highly variable (Peng *et al.*, 1979; Hasse and Liss, 1980). For simplicity, the mean value of 36μ was adopted for our calculation. The exchange coefficient was calculated to be 5.8 m/day, which is consistent with the observed mean exchange coefficient within 20-40°N in the Pacific Ocean (Peng *et al.*, 1979). Then, the oxygen flux was computed to be 0.07 mol/m^2/day. There were two other stations (5220 and 5121) on transect A, where undersaturation of oxygen was observed in the surface water. The oxygen fluxes were calculated to be 0.08-0.09 mol/m^2/day. There were two ways to maintain the oxygen undersaturation at the surface: by downward diffusion of oxygen from the surface water to the subsurface water or by upward advection (upwelling) of oxygen-depleted water. If the vertical mixing is the dominant process for maintaining the surface oxygen deficiency, the vertical eddy diffusivity can be calculated. The vertical oxygen gradient in the top layer (0-10m) was -0.37μM/m. If the surface balance was maintained by diffusion only, the vertical diffusivity was calculated to be 21 cm^2/s by Fick's first law of diffusion, under the assumption of no production or consumption of oxygen. It will be shown later that the biological effect on oxygen within the surface layer of about 10 m is negligible in comparison with the diffusive flux. Similarly, the vertical diffusivity was calculated to be 10-25 cm^2/s for the two stations on transect A. The mean vertical diffusivity was 19 cm^2/s, which is reasonable for the surface boundary layer (Gargett, 1984).

For the middle layer of sta. 5521, the oxygen gradient was -0.47μM/m. If the downward transport of the surface oxygen flux was maintained only by vertical diffusion, the diffusivity was calculated to be 16 cm^2/s. This value is too large because the normal eddy diffusivity for the interior of the water body is about an order of magnitude lower (Gargett, 1984). Therefore, other processes should be important in maintaining the oxygen deficiency in the middle layer. One alternative mechanism is upwelling of oxygen-depleted water from below. A simple box model is invoked to estimate the upwelling velocity in the following.

4.5 A Simple Box Model for Upwelling

Because the upwelling center is a cold eddy (Chern *et al.*, 1990), it should be a rather isolated water body and could be treated as a box. The box defined in the model depicted in Figure 11 represented the upper half of the upwelling dome, which included the top and middle layers, i.e., the upper 60m, of the water column shown in Figure 10. Below this depth the vertical gradients of temperature and oxygen were small, so that the vertical diffusion may be neglected. The lateral boundaries of the box were set to be the four sides of the trapezoid defined by stations 5315 and 512A on transect A and stations 5521 and 5323 on

transect B, which had an area of 2900km^2. In the cross-shelf direction, main body of the upwelling dome was bracketed within the boundaries, but in the along-shelf direction the available data were not enough to cover the full extent of the upwelling dome. Therefore, the box only represented the minimum extent of the upwelling dome. The parameters and arithmetic of the model calculation are described in detail in the Appendix. The method for evaluation of the parameters was also explained.

The case observed on the March cruise was used for calculation of the upwelling velocity because the lateral mixing processes may be simplified. The sharp salinity boundary between the inner shelf water and the upwelling dome (Figure 4) suggested that the lateral exchange between the two waters was restricted. Therefore, we assumed that the lateral exchange only occurred between the upwelling dome and the Kuroshio Water.

The exchange of water in the box with its surroundings was achieved by upwelling, lateral mixing or advection. The bottom layer of the upwelling dome was quite uniform in terms of oxygen distribution. In this model, the upwelling velocity, which was assumed to have a mean value of W, represented the vertical velocity of water transported from the bottom layer to the upper layer within the upwelling region. To balance mass, the upwelled water was assumed to exit the box through horizontal advection. The lateral exchange was assumed to have a mean transport of X between the box and the top 60m of the Kuroshio Water (Figure 11).

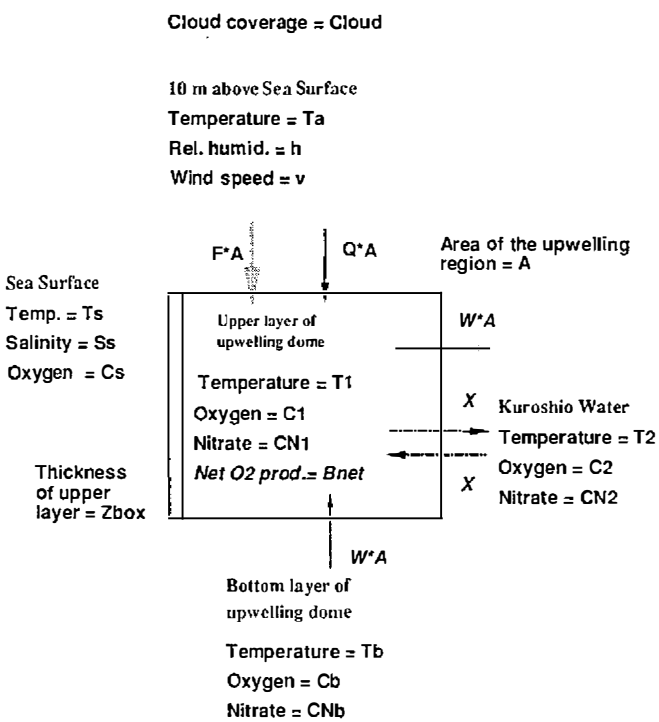

Fig. 11. The box model for calculation of the upwelling velocity. Thermal balance and mass balance of water, oxygen and nitrate were considered for the model. The lateral processes were assumed to occur between the upwelling dome and the Kuroshio Water only. The double vertical line on the left side of the box indicates no exchange with the inner shelf water. The parameters in Italic style represent unknowns. See text and Appendix for detail of the model.

Under steady state condition, the inputs of heat or material were balanced by the outputs. We assumed that the water transported in and out of the box had fixed temperature and oxygen concentrations. The water in the upper layer of the upwelling region had the mean properties: T = 19.7°C and $[O_2]$ = 208 μM. The upwelled water was assumed to have the properties of the water from depths of 60-80m just beneath the box: T = 17.8 °C and $[O_2]$ = 194 μM. The water from the upper 60m of the Kuroshio Water had the mean properties: T = 23.8°C and $[O_2]$ = 217 μM.

In addition to fluxes associated with the water transports, there were oxygen and thermal fluxes from above the sea surface. The mean oxygen flux was calculated by equation (1). The mean oxygen concentration in surface water in the upwelling area was 221μM, and the saturated concentration was calculated to be 228μM for the mean temperature of 20.87°C and mean salinity of 34.47 psu. The downward flux of oxygen was then calculated to be 0.39×10^{-6} mol/m^2/s (0.034 mol/m^2/day), under the same assumption of 36μ for the thickness of the surface laminar layer. It is noted that the center of the upwelling dome could be between the two transects and missed by the sampling stations as indicated by the satellite imagery of the sea surface temperature during the September cruise (Liu *et al.*, 1992). If the same situation occurred in March, then the estimated oxygen would be an underestimation.

The thermal flux at sea surface was more complicated to calculate than the oxygen flux (see Appendix for detail). It consists of several components, namely the solar heating, heat loss from longwave radiation, evaporation, and sensible heat flux. The solar radiation is measured at some but not all weather stations. For our calculation, we used the mean value (115 W/m^2) of global solar radiation data measured during March 4-9, 1990 at the Ilan Weather Station of the Central Weather Bureau. The other heat fluxes can be calculated from the sea surface temperature, and the temperature, humidity, wind speed and cloud coverage over the sea surface (Pickard and Emery, 1990). The mean air temperature (21.7°C) and wind speed (6.4 m/s) in the upwelling region were obtained from ship board measurement. The relative humidity (93.5%) and cloud coverage (85%) were adopted from the mean values measured at Pengchia Yu by the CWB. The mean sea surface temperature (20.87°C) of the upwelling region was calculated from the CTD data. The calculated values for the net thermal flux to the water at the sea surface was: 98 W/m^2.

Oxygen concentration in seawater is affected not only by physical processes but also by biological processes. It is produced during photosynthesis and consumed during respiration. Both processes involve nitrate transformation in the opposite direction. In the model, the net oxygen productivity was assumed proportional to the net consumption rate of nitrate which was in turn calculated from the nitrate budget. The Redfield ratio, 8.6, for $O_2/(-NO_3^-)$ was used as the proportional constant (Redfield *et al.*, 1963).

The model calculation yielded an upwelling velocity of 6.3×10^{-5} m/s (or 5.4 m/day), which corresponded to an upwelling transport of 0.2 Sv into the box. If the upwelling was supported by bottom intrusion with a thickness of 50m along the bottom, the shelfward velocity would be 7.2 cm/s within the width (50.8km) of the P-box. The calculation also showed that the oxygen flux from the atmosphere was almost as important as the net oxygen input from lateral exchange, whereas the thermal flux from above was less than one half of the net thermal flux from lateral exchange. The turnover time of the water in the box was calculated to be 8 days. About 3/4 of the water replacement was attributed to upwelling. The upwelling velocity implied an nutrient flux of 0.04 mol N/m^2/day, which amounted to a transport of about 1750 metric tons of nitrogen as nitrate to the box daily. Such a transport

was much stronger than the daily mean transport of 100-360 metric tons estimated for the southeastern U.S. continental shelf during events of Gulf Stream intrusion (Lee *et al.*, 1981; Atkinson *et al.*, 1984).

Because the area and the degree of oxygen undersaturation in the surface water of the upwelling region were both lower limits, the upwelling velocity and transport should also be underestimated. However, the model had many assumptions which may lead to considerable uncertainties in the results. Most notably, the steady state assumption may not be representative of the transient state, keeping in mind that considerable temperature fluctuation with a range up to 3°C over a week was observed by the mooring at 190 m-depth at station W (NSC, 1991). Secondly, the temperature and chemical properties of the waters transported in or out of the box were not as uniform as suggested by the model. Thirdly, the lateral water exchange across the strong salinity front between the upwelling dome and the inner shelf water was neglected in the model, but, in reality, it might not be negligible. Finally, the water properties showed considerable spatial variation so that the sampling stations were probably not close enough to capture all the essential features.

The model calculation also predicted a net oxygen productivity to be 0.26×10^{-6} mol/m^2/s, which warranted further comparison with other measurements. The primary productivity in the sea off northern Taiwan has been measured to be 1.1 ± 0.6 gC/m^2/day in the spring (Hung *et al.*, 1980), which corresponds to an oxygen productivity of $(1.3 \pm 0.7) \times 10^{-6}$ mmol/m^2/s under the assumption of an $O_2/(-CO_2)$ ratio of 1.2 during photosynthesis (Ryther, 1965). If the oxygen productivity in the study area was similar to this value, only 20% of produced oxygen in photosynthesis survived respiration in the top 60m. The flux of oxygen consumption in the box was calculated to be 1.0×10^{-6} mol/m^2/s, which corresponds to an average rate of 1.6×10^{-8} mol/m^3/s. This value is comparable to the oxygen consumption rate of $(1.4 \pm 1.0) \times 10^{-8}$ mol/m^3/s for the surface water in the Peru upwelling region (Packard *et al.*, 1983). The net oxygen production calculated from the model also supported the assumption of insignificant biological effect on oxygen in the surface layer for the calculation of the diffusion coefficient in the last section. For the surface layer of 10m, the net oxygen production would be about 0.05×10^{-6} mol/m^2/s, which was considerably less than the mean diffusive flux of 0.39×10^{-6} mol/m^2/s.

In addition, sensitivity tests were made by varying the heat or oxygen fluxes at sea surface, which were obtained by calculation rather than from observation and, therefore, are the most uncertain. An increase or decrease by 50% of the fluxes yielded variation in the resultant upwelling velocity by less than 35%. If the upwelling water was assumed to have the mean properties of the water from 60-120m beneath the box, the resultant upwelling velocity was lower by about 20%, suggesting that the choice of these parameters was not overly sensitive. The significance of the lateral exchange with the inner shelf water was also investigated by calculating the intensity of the lateral exchange between the upwelling dome and the inner shelf water needed to balance the salt budget, which was not considered in our model calculation. The results showed that the transport was less than 1/3 of that between the upwelling dome and the Kuroshio Water but the contribution to the oxygen input could be as important as the other sources. If this extra flux was included in the model, the estimated upwelling velocity would increase by about 30%. Because the frontal salinity gradient was too great to be resolved by the sampling stations, the salt budget was not likely to be balanced with sufficient accuracy. Model deficiencies aside, the estimated upwelling velocity should be correct within a factor of 2.

To improve further, intensive observation, both in terms of time and space, is needed to better define the temporal and spatial variation of the water properties within and surround the upwelling dome. Direct measurement of primary productivity and grazing rate will help to determine the biological effect on oxygen budget more precisely. The limiting time scale for our model was the oxygen exchange rate at the sea surface. In this regard, a better tracer for studying the air-sea exchange process is ^{222}Rn (e.g., Broecker and Peng, 1974), which has a half life of 3.8 days, and, therefore, is ideally suited for a system with a turnover time of about a week. Finally, the horizontal circulation pattern in the study region should be better defined to construct a more realistic model.

5. SUMMARY AND CONCLUSIONS

Monthly hydrographic survey in the KEEP study area during August 1990 - July 1991 indicated that upwelling dome existed all year around. When temperature or nitrate distributions failed to distinguish the upwelled water from the shelf water in March and April 1991, dissolved oxygen served the purpose rather nicely. The cold and high-oxygen shelf water readily contrasted with the oxygen-depleted upwelled water during that period. The upwelling domes showed more or less symmetric structure with respect to the shelf break throughout the year, except during episodes of onshore movement of the Kuroshio onto the East China Sea in October and April. When horizontal intrusion occurred, the shelfward half of the dome structure showed isopleths almost parallel to the sea floor. During two cruises, a secondary dome was observed. The center of upwelling stayed fairly fixed at the shelf break with only slight oscillation, suggesting a locking effect probably controlled by bottom topography. The surface shelf water was rich in nitrate during the NE monsoon period. When the shelf water outflowed as filaments, it could provide the barren surface water of the open sea with nutrients.

The upwelling center was undersaturated with oxygen from December to May. A box model was invoked to simulate the undersaturation process observed in March 1991. The mean downward flux of oxygen from the atmosphere to the surface seawater was estimated to be 0.034 mol/m^2/day. Considering the balance of heat, oxygen and nitrate, and biological activities relating the last two, we calculated an upwelling velocity of about 5 m/day to maintain a steady state in the upper 60m of the upwelling dome. For the upwelling area of 2900km^2, the total upwelling transport was about 0.2 Sv, and the nitrate transport was about 2×10^9 gN/day.

Acknowledgments This is a contribution (IESEP92-021) from the Institute of Earth Sciences, Academia Sinica (ROC). We acknowledge the cooperation of the crew and technical staff of the R/V Ocean Researcher I during our cruises. Special thanks are due to Dr. T.-Y. Tang of the Institute of Oceanography, NTU, Mr. J.-Y. Chen of the Central Weather Bureau and Dr. C.-Z. Shyu of the Taiwan Fisheries Research Institute for providing wind plots, meteorological data and satellite SST images, respectively. This manuscript was improved by numerous comments and constructive suggestions from Drs. S.-Y. Chao and C.-T. Liu and two reviewers. We are especially grateful for the assistance of S.-J. Tung, P.-H. Cheng, P. Chen, Y.-J. Lee, W.-R. Yang, Y.-H. Wen, C.-S. Oun, and T.-Y. Kuo. This study was supported by grants from the National Science Council of the Republic of China: 81-0209-M001-01 (KKL), 80-0209-M002a-14 (SL), 80-0209-M002a-12 (CYY), 80-0209-M002a-13

(CLW), 80-0209-M002a-20 (SCP) and 80-0209-M110-01 (CKW), and also by Academia Sinica.

REFERENCES

Atkinson, L.P., 1977: Modes of Gulf Stream intrusion into the South Atlantic Bight shelf waters. *Geophys. Res. Lett.* **4**, 583-586.

Atkinson, L.P., 1985: Hydrography and nutrients of the southeastern U.S. continental shelf. In: Atkinson, L.P. , D.W. Menzel and K.A. Bush (eds), *Oceanography of the Southeastern U.S. Continental Shelf*, American Geophysical Union, Washington, D.C., 77-92.

Atkinson, L.P., P.G. O'Malley, J.A. Yorder and G.A. Paffenhoffer, 1984: The effect of summertime shelf upwelling on nutrient flux in southeastern United States continental waters. *J. Mar. Res.*, **42**, 969-993.

Brink, K.H., 1987: Coastal ocean physical processes. *Rev. Geophys.* **25**, 204-216.

Broecker, W.S. and T.H. Peng, 1974: Gas exchange rates between air and sea. *Tellus*, **26**, 21-35.

Csanady, G.T., 1990: Physical basis of coastal productivity. *Eos Trans., AGU*, **71**, 1060-1065.

Carpenter, J. 1965: The Chesapeake Bay Institute technique for the Winkler dissolved oxygen method. *Limnol. Oceanogr.* **10**, 141-143.

Chen, Y.-L., 1992: The primary producers in the KEEP area (Extended abstract). KEEP & WOCE Conference, Feb. 26-29, 1992, Nantou, Taiwan, ROC.

Chern, C.S. and J. Wang, 1989: On the water masses at northern offshore area of Taiwan. *Acta Oceanographica Taiwanica*, No. **22**, 14-32.

Chern, C.S. and J. Wang, 1990: On the mixing of waters at a northern offshore area of Taiwan. *TAO*, **1**, 297-306.

Chern, C.S., J. Wang and D.P. Wang, 1990: The exchange of Kuroshio and East China Sea shelf water. *J. Geophys. Res.*, **95**, 16017-16023.

Chuang, W.S. and C.K. Wu, 1992: Slope current fluctuations northeast of Taiwan, winter 1990. *J. Oceanogr. Soc. Jap.*, **47**, 185-193.

Craig, H., W.S. Broecker and D. Spencer, 1981: GEOSECS Pacific Expedition. National Science Foundation, Washington D.C., USA.

Dunstan, W.M. and L.P. Atkinson, 1976: Sources of new nitrogen for the South Atlantic Bight. In: I.M. Wiley (ed.), *Estuarine Processes*, pp. 69-98, Academic Press, N.Y.

Edmond, J.M., A. Spivack, B.C. Grant, M.-H. Hu, Z. Chen, S. Chen and X. Zeng, 1985: Chemical dynamics of the Changjiang estuary. *Continental Shelf Res.*, **4**, 17-36.

Fan, K.L., 1980: On upwelling off northeastern shore of Taiwan. *Acta Oceanographica Taiwanica*, **No. 11**, 105-117.

Fujian Institute of Oceanology, 1988: A comprehensive oceanographic survey of the central and northern part of the Taiwan Strait. China Science Press, 423 pp.

Gardner, W.S., D.S. Wynne and W.M. Dunstan, 1976: Simplified procedure for the manual analysis of nitrate in seawater. *Mar. Chem.* **4**, 393-396.

Gargett, A.E., 1984: Vertical eddy diffusivity in the ocean interior. *J. Mar. Res.*, **47**, 359-393.

Gong, G.C. and K.K. Liu, 1991: Kuroshio Edge Exchange Processes: hydrography sections, August 1990 - July 1991. R/V Ocean Researcher I Regional Instrument Center, National Science Council, Taipei, ROC.

Gong, G.C., K.K. Liu and S.C. Pai, 1991: Nitrate-temperature relationship in the Kuroshio and adjacent seas surrounding Taiwan. Proceed. Conf. on Physical and Chemical Oceanography of the China Seas, Hangzhou, June 25-29, 1991.

Goody, R.M. and J.C.G. Walker, 1972: Atmospheres. Prentice-Hall, Englewood Cliffs, N.J., USA. 150 pp.

Hasse, L. and P.S. Liss, 1980: Gas exchange across air-sea interface. *Tellus*, **32**, 470-481.

Hung, T.-C., S.-H. Lin and A. Chuang, 1980: Relationships among particulate organic carbon, chlorophyll-a and primary productivity in sea water along the northern coast of Taiwan. *Acta Oceanographica Taiwanica*, **No. 11**, 70-88.

Hwang, S.-J. and T.-Y. Tang, 1992: Distribution of CTD observations, distribution of winds, vertical profiles of temperature, salinity, density. CTD Data Bank Data Report, Vol. I, Regional Instrument Center, R/V Ocean Researcher I, National Science Council, Taipei, Taiwan, ROC.

Kester, D., 1975: Dissolved gases other than CO2. In: J.P. Riley and G. Skirrow (ed.) *Chemical Oceanography*, 2nd ed., Vol. 1, pp. 498- 556, Academic Press, London.

Kumpferman S.L. and N. Garfield, 1977: Transport of low salinity water at the slope water-Gulf Stream boundary. *J. Geophys. Res.* **82**, 3481-3486.

Lee, D., 1992: A study on the vertical structure of the semi-diurnal tide at the shelf break off northeastern Taiwan. M.S Thesis, Inst. Oceanogr., National Taiwan Univ., 108 pp.

Lee, T.N., L.P. Atkinson, and R. Legeckis, 1981: Detailed observation of a Gulf Stream spin-off eddy on the Georgia Continental shelf, April, 1977. *Deep-Sea Res.*, **28**, 347-378.

Liu, C.T. and S.C. Pai, 1987: As the Kuroshio turns: (II) The oceanic front north of Taiwan, *Acta Oceanographica Taiwanica*, **No. 18**, 49-61.

Liu K.K., G.C. Gong, C.Z. Shyu, S.C. Pai, C.L. Wei, and S.Y. Chao , 1992: Response of Kuroshio upwelling to the onset of northeast monsoon in the sea north of Taiwan: observations and a numerical simulation. *J. Geophys. Res.* **97**, 12511-12526.

Liu, K.K., S.C. Pai and C.T. Liu, 1988: Temperature-nutrient relationships in the Kuroshio and adjacent waters near Taiwan, *Acta Oceanographica Taiwanica*. **No. 21**, 1-17.

Luther, M.E. and J.M. Bane, 1985: Mixed instability in the Gulf Stream over the continental slope. *J. Phys. Oceanogr.* **15**, 3-23.

Miao, Y. and H. Yu, 1990: Spatial and temporal variation of water mass mixing characteristic in the East China Sea, in Proceed. Japan- China Joint Symposium of the Cooperative Study on the Kuroshio, Nov. 14-16, 1989, Tokyo, Japan, pp. 157-169, Science and Technology Agency, Tokyo, Japan.

NSC, 1991: KEEP Moorings (1990.10 - 1991.8), Physical Oceanographic Data Bank Data Report, Vol. 1. Regional Instrument Center R/V Ocean Researcher I, National Science Council, Taipei, Taiwan, ROC.

Pai, S.C., G.C. Gong, and K.K. Liu, 1992: Determination of dissolved oxygen in seawater based on direct spectrophotometry of total iodine. *Mar. Chem.* (In press).

Pai, S.C., C.C. Yang and J.P. Riley, 1990: Formation kinetics of the pink azo dye in the determination of nitrite in natural waters. *Anal. Chim. Acta* **232**, 345-349.

Parsons, T.R., M. Takahashi and B. Hargrave, 1984: Biological Oceanographic Processes, 3rd. ed. Pergamon Press, 330 pp.

Packard, T.T., P.C. Garfield and L.A. Codispoti, 1983: Oxygen consumption and denitrification below the Peruvian upwelling, In: E. Suess and J. Thiede (eds.), *Coastal Upwelling*, Part A, pp. 147-174, Plenum Press, NY.

Pickard, G.L. and W.J. Emery, 1990: *Descriptive Physical Oceanography*, 5th Ed. Pergamon Press, Oxford, 320 pp.

Peng, T.-H., W.S. Broecker, G.G. Mathieu, and Y.-H. Li, 1979: Radon evasion rates in the Atlantic and Pacific Oceans as determined during the Geosecs program. *J. Geophys. Res.*, **84**, 2471-2486.

Redfield, A.C., B.H. Ketchum and F.A. Richards, 1963: The influence of organisms on the composition of seawater. In: M.N. Hill *et al.* (eds), *The Sea*, Vol. 2, pp. 26-49, Wiley, N.Y.

Ryther, J.H., 1965: The measurement of primary production, *Limnol. Oceanogr.* **1**, 72-84.

Strickland, J.D.H. and T.R. Parsons, 1972: *A Practical Handbook of Seawater Analysis.* pp. 71-76. Bulletin 167 (2nd ed.), Fisheries Research Board of Canada, Ottawa.

Su, J. and Y. Pan, 1987: On the shelf circulation north of Taiwan. *Acta Oceanologica Sinica*, **6**, Supp. I, 1-20.

Takahashi, M., I. Koike, T. Ishimaru, T. Saino, K. Furuya, Y. Fujita, A. Hattori and S. Ichimura, 1980: Upwelling plumes in the Sagami Bay and adjacent water around the Izu Islands, Japan. *J. Oceanogr. Soc. Jap.* **36**, 209-216.

Tang, T.-Y. and J.-Y. Chen, 1990: National Science Council R/V Ocean Research I Hydrography Report, Vol. II, Inst. of Oceanogr., National Taiwan University, pp.18-19.

Walsh, J.J., 1991: Importance of continental margins in the marine biogeochemical cycling of carbon and nitrogen. *Nature* **350**, 53- 55.

Walsh, J.J., P.E. Biscaye and G.T. Csanady, 1988: The 1983-1984 Shelf Edge Exchange Processes (SEEP)-I experiment: hypotheses and highlights. *Cont. Shelf Res.*, **8**, 435-456.

Wanninkhof, R. J.R. Ledwell and W.S. Broecker, 1985:. Gas-exchange- wind speed relation measured with sulfur hexafluoride on a lake. *Science*, **227**, 1224-1226.

Weiss, R.F., 1970: The solubility of nitrogen, oxygen and argon in water and seawater. *Deep-Sea Res.*, **17**, 721-735.

Wong, G.T.F., S.C. Pai , K.K. Liu , C.T. Liu and C.T.A. Chen, 1991: Variability of the chemical hydrography at the frontal region between the East China Sea and the Kuroshio north-east of Taiwan. *Estuarine Coastal Shelf Sci.* **33**, 105-120.

Wroblewski, J.S. and E.E. Hofmann , 1989: U.S. interdisciplinary modeling study of coastal-offshore exchange processes: past and future. *Prog. Oceanogr.* **23**, 65-99.

Yorder, J.A., L.P. Atkinson, S.S. Bishop, E.E. Hofmann and T.N. Lee , 1983: Effect of upwelling on phytoplankton productivity on the outer southeastern U.S. continental shelf. *Continent. Shelf Res.*, **1**, 385-404.

Appendix. Arithmetic of the Box Model

A box model was used to calculate the upwelling velocity of the bottom water to the upper layer in the upwelling region (Figure 11). The box represented the upper layer which is assumed to be at a steady state with respect to nitrate and oxygen concentrations and temperature. Mass balance and thermal balance were used to calculate the upwelling flux and the lateral transport needed to balance the oxygen and thermal fluxes from above. The net oxygen production was calculated from the nitrate consumption rate needed to balance the nitrate fluxes. Upwelling is the only vertical water transport; all other water transports are lateral exchange with the Kuroshio Water.

The input and output parameters used in the model are listed in Tables A-1 and A-2, respectively. The equations for balance of heat, oxygen and nitrate are as the following:

Table A-1. Input parameters of the box model

Parameters (unit)	Description
A (m^2)	Area of the upwelling region (UR)
C1 (mol/m^3)	Mean [O_2] of the box (upper layer of the UR)
C2 (mol/m^3)	Mean [O_2] in the upper Kuroshio Water
Cb (mol/m^3)	Mean [O_2] in the bottom layer of the UR
Cloud (oktas)	Cloud coverage (0-8)
CN1 (mol/m^3)	Calculated mean nitrate concentration in the box
CN2 (mol/m^3)	Mean [NO_3^-] in the upper Kuroshio Water
CNb (mol/m^3)	Mean [NO_3^-] in the bottom layer of the UR
Cp (J/m^3)	Volumetric heat capacity of seawater at normal pressure
Cs (mol/m^3)	[O_2] at the sea surface (SS) of the UR
DO2 (m^2/s)	Molecular diffusivity of oxygen at SS
Film (m)	Film thickness of gas exchange at SS
h (%)	Relative humidity at 10 m above SS
Pwa (kPa)	Vapor pressure at 10 m above SS
Pws (kPa)	Vapor pressure at SS
Qsolar (W/m^2)	Heat flux to the sea from solar radiation
Rr	Redfield ratio of O_2/NO_3 = 8.6
T1,T2,Ta,Tb (°C)	Same as C1, C2 etc., except for temperature(°C)
Ts,Ss	Temperature (°C) and salinity (psu) at SS
v (m/s)	Wind velocity at 10 m above SS
Zbox (m)	Thickness of the box (upper layer of the UR)

Table A-2. Output parameters of the box model

Parameters (unit)	Description
Bnet (mol/m^2/s)	Net input of oxygen from biological activities
Csat (mol/m^3)	Solubility of oxygen at SS
F (mol/m^2/s)	Oxygen flux at SS
fOX	Fraction of contribution of F to the total oxygen flux to the box except upwelling
bOX	Fraction of biological contribution in total oxygen flux to the box except upwelling
fQ	Fraction of contribution of Q in total heat flux to the box except upwelling
Q (W/m^2)	Heat flux to the box at SS
Qcon (W/m^2)	Conduction heat flux at SS
Qlat (W/m^2)	Latent heat flux (evpor., condensat.) at SS
Qrad (W/m^2)	Radiative (long wavelength) heat flux at SS
Tau (s)	Residence time of seawater in the box
rUP	Fraction of contribution of upwelling in water exchange
UP (m^3/s)	Transport of upwelling into the box
W (m/s)	Upwelling velocity
X (m^3/s)	Volume transport of lateral water exchange

$$Q \times A + Cp(Tb - T1) \times W \times A + Cp(T2 - T1)X = 0, \quad (A1)$$

$$F \times A + (Cb - C1) \times W \times A + (C2 - C1)X + Bnet \times A = 0, and \quad (A2)$$

$$(CNb - CN1) \times W \times A + (CN2 - CN1)X + Bnet \times A/Rr = 0, \quad (A3)$$

where Q is calculated from the different components of the heat budget as suggested by Pickard and Emery (1990):

$$Q = Qsolar + Qrad + Qcond + Qlat \quad (A4)$$

The value of each component was either measured or calculated from the sea surface conditions and meteorological data. The global solar radiation was taken from meteorological data of the Central Weather Bureau. The other values were estimated from the following relationships:

$$Qrad = -(143 - 0.9Ts - 0.46h)(1 - 0.1Cloud) \quad (A5)$$

$$Qcond = 1.88v(Ta - Ts) \quad (A6)$$

$$Qlat = -1.4(Pws - Pwa)v(2494 - 2.2Ts) \quad (A7)$$

The solutions for W, X and Bnet are as follows.

$$\begin{aligned} W =&(-F + Q((C2 - C1) + Rr(CN2 - CN1))/(T2 - T1)/Cp)/ \\ &((Cb - C1) + Rr(CNb - CN1) \\ &- ((C2 - C1) + Rr \times (CN2 - CN1)) \times (Tb - T1)/(T2 - T1)) \end{aligned} \quad (A8)$$

$$X = -A \times ((Tb - T1) \times W + Q/Cp)/(T2 - T1) \quad (A9)$$

$$Bnet = Rr \times ((CNb - CN1) \times W + (CN2 - CN1) \times X/A) \quad (A10)$$

The upwelling transport and the residence time of the water in the box were calculated by the equations:

$$\begin{aligned} UP &= W \times A \\ Tau &= A \times Zbox/(X + UP). \end{aligned} \quad (A11)$$

The significance of upwelling to the turnover of water in the box was calculated as follows.

$$rUP = W \times A/(X + UP) \quad (A12)$$

The contribution of the thermal and oxygen fluxes from above the sea surface in the total input fluxes other than upwelling were calculated according to the following relationships.

$$fOX = F/(F + p - R \times Zbox + (C2 - C1) \times X/A) \quad (A13)$$

$$fQ = Q \times A/(Q \times A + (T2 - T1) \times X \times Cp) \quad (A14)$$

The importance of the biological activities in the total input flux of oxygen other than upwelling was calculated according to the following relationships.

$$bOX = fOX \times (p - R \times Zbox)/F \quad (A15)$$

The values of input parameters and the results of calculation are listed in Table A-3. The value of each hydrographic and chemical parameter was estimated by averaging the integrated means along the two transects. For the values within the box and below the box, the stations from 5315 to 512A along transect A and from 5521 to 5323 along transect B were used for evaluation (Figure 1). For the parameters of the Kuroshio Water, the stations from 5022 to 4430 along transect A and from 5224 to 4531 along transect B were used for evaluation.

Table A-3. Values of input and output of the box model

Input parameters	Input values	Output parameters	Output values
A (m^2)	$2.9x10^9$	Bnet ($mol/m^2/s$)	$0.26x10^{-6}$
C1 (mol/m^3)	0.208	Csat (mol/m^3)	0.228
C2 (mol/m^3)	0.217	F ($mol/m^2/s$)	$0.39x10^{-6}$
Cb (mol/m^3)	0.194	fOX	0.46
Cloud (oktas)	6.8	bOX	0.30
CN1 (mol/m^3)	$5.56x10^{-3}$	fQ	0.21
CN2 (mol/m^3)	$0.26x10^{-3}$	Q (W/m^2)	97.5
CNb (mol/m^3)	$7.92x10^{-3}$	Qcon (W/m^2)	10
Cp (J/m^3)	$3.9x10^6$	Qlat (W/m^2)	-1.6
Cs (mol/m^3)	0.221	Qrad (W/m^2)	-26
DO2 (m^2/s)	$2.04x10^{-9}$	Tau (s)	$7.0x10^5$
Film (m)	$3.0x10^{-5}$	rUP	0.74
h (%)	93.5	UP (m^3/s)	$0.18x10^6$
Pwa (kPa)	2.51	W (m/s)	$0.63x10^{-4}$
Pws (kPa)	2.42	X (m^3/s)	$0.65x10^5$
Qsolar (W/m^2)	115		
T1 (°C)	19.67		
T2 (°C)	23.85		
Ta (°C)	21.70		
Tb (°C)	17.79		
Ts (°C)	20.87		
Ss (psu)	34.47		
V (m/s)	6.4		
Zbox (m)	60		

臺灣北部外海大陸棚緣湧升流之全年化學水文觀測

劉康克[1,2]、龔國慶[2,3]、林曉武[2]、楊肇岳[2]
魏慶琳[2]、白書禎[2]、吳重坤[4]

1. 中央研究院地球科學研究所
2. 國立臺灣大學海洋研究所
3. 國立臺灣海洋大學海洋系
4. 國立中山大學海洋資源系

摘要

臺灣北部大陸棚邊緣有湧升流，這是黑潮與東海陸棚接觸後所產生的一個重要的物理現象，並造成明顯的化學及生物變化。過去經常觀察到在海面上有一片異常冷之水域，即湧升區。然而，此種溫度的對比並不一定常年存在，因爲陸棚水在冬季會變冷，甚至比湧升區之水溫更低。因此，以往並沒有全年的資料顯示湧升流是經常存在的。從1990年8月到1991年7月，本研究執行了十一次的海上探測，由溫度、硝酸鹽及溶氧的分布顯示，湧升流的確經年存在著。當冬季溫度及硝酸鹽的分布無法顯示湧升流的全貌時，溶氧是一個特別有用的指標，它顯示冬季時湧升流的丘狀構造與其它季節相似。在十二月至五月間，湧升區的表水都有溶氧不飽和的現象。利用一個盒式模型可估計，在1991年 3月間湧升區的平均溶氧速率約爲0.034 莫耳/平方公尺/天。如要維持表層海水的不飽和，它必須以每天 5 公尺的速率被下層海水所取代。在面積爲2900平方公里的湧升區內，總湧升流量約爲 0.2 Sv，所攜帶的硝酸根爲2×10^9公克氮/天。